Metallic atomically-thin layered silicon epitaxially grown on silicene/ZrB$_2$

You may also be interested in:

Progress in the materials science of silicene
Yukiko Yamada-Takamura and Rainer Friedlein

Electronic properties of epitaxial silicene on diboride thin films
Rainer Friedlein and Yukiko Yamada-Takamura

Two dimensional silicon: the advent of silicene
Carlo Grazianetti, Eugenio Cinquanta and Alessandro Molle

A theoretical review on electronic, magnetic and optical properties of silicene
Suman Chowdhury and Debnarayan Jana

Epitaxial growth of silicene on ultra-thin Ag(111) films
Junki Sone, Tsuyoshi Yamagami, Yuki Aoki et al.

Silicene: a review of recent experimental and theoretical investigations
M Houssa, A Dimoulas and A Molle

Multilayer silicene: clear evidence
Paola De Padova, Amanda Generosi, Barbara Paci et al.

2D Materials

CrossMark

LETTER

Metallic atomically-thin layered silicon epitaxially grown on silicene/ZrB₂

Tobias G Gill[1,2,3], Antoine Fleurence[3], Ben Warner[1,4], Henning Prüser[1], Rainer Friedlein[3,6], Jerzy T Sadowski[5], Cyrus F Hirjibehedin[1,2,4] and Yukiko Yamada-Takamura[3]

1 London Centre for Nanotechnology, University College London (UCL), London WC1H 0AH, United Kingdom
2 Department of Chemistry, UCL, London WC1H 0AJ, United Kingdom
3 School of Materials Science, Japan Advanced Institute of Science and Technology, Nomi, Ishikawa 923-1292, Japan
4 Department of Physics and Astronomy, UCL, London WC1E 6BT, United Kingdom
5 Center for Functional Nanomaterials, Brookhaven National Laboratory, Upton, NY 11973, United States of America
6 Current address: Meyer Burger (Germany) AG. An der Baumschule 6-8, 09337 Hohenstein-Ernstthal, Germany

E-mail: toby.gill.09@ucl.ac.uk, c.hirjibehedin@ucl.ac.uk and yukikoyt@jaist.ac.jp

Keywords: silicene, scanning tunnelling microscopy (STM), low energy electron diffraction (LEED), silicon nanostructures

Supplementary material for this article is available online

Abstract

Using low energy electron diffraction (LEED) and scanning tunnelling microscopy (STM), we observe a new two-dimensional (2D) silicon crystal that is formed by depositing additional Si atoms onto spontaneously-formed epitaxial silicene on a ZrB₂ thin film. From scanning tunnelling spectroscopy (STS) studies, we find that this atomically-thin layered silicon has distinctly different electronic properties. Angle resolved photoelectron spectroscopy (ARPES) reveals that, in sharp contrast to epitaxial silicene, the layered silicon exhibits significantly enhanced density of states at the Fermi level resulting from newly formed metallic bands. The 2D growth of this material could allow for direct contacting to the silicene surface and demonstrates the dramatic changes in electronic structure that can occur by the addition of even a single monolayer amount of material in 2D systems.

1. Introduction

Silicene, a honeycomb lattice of Si atoms, has been predicted to share many interesting properties with its carbon counterpart, graphene [1]. Unlike graphene, however, the triangular sublattices of free-standing silicene are displaced out-of-plane with respect to one another [2–4]. As a consequence, the electronic structure of free-standing silicene is likely to be more susceptible to modification by external fields. Due to this, and the greater spin orbit coupling in Si resulting in a relatively large spin–orbit bandgap of 1.55 meV [3, 4], silicene's electronic properties may prove useful in nanoscale device fabrication [5–8]. Recent work has shown that silicene can be incorporated into a conventional field-effect transistor architecture [9], a process that involves the complex etching of metallic contacts on the delicate silicene surface. It is therefore desirable to develop new techniques for patterning conductive contacts onto two-dimensional (2D) materials at the nanoscale.

To date, silicene has been grown upon a number of metallic substrates [10–15]. As with graphene [16–20],

interactions with the underlying substrate are expected to play a significant role in enabling the tuning of the electronic properties [21]. In particular, when placed upon a surface, the specific buckling of the silicene lattice is heavily influenced by interactions with the substrate [10–15, 22]. For many layered materials, such as graphene [23–25] and various transition metal dichalcogenides like MoS₂ [26, 27], it has previously been observed that the electronic and electro-optic properties can change dramatically when going from the mono- to multi-layer regime. Similarly, multi-layered silicene is predicted to exhibit a broad range of interesting physical phenomena including a tunable bandgap [28], superconductivity [29], and behaviour as a quasi-topological insulator [30]. Recent experiments studying multiple Si layers deposited on Ag (1 1 1) show that an additional Si layer can change the surface reconstruction [31], and even more dramatically the electronic properties. In particular, as the number of Si layers is increased, the tunnelling conductance is found to decrease [32]. While other studies have highlighted strong similarities to the Ag-terminated Si (1 1 1) surface [33, 34], the substrate

temperature during deposition may be key to determining the formation of either an Ag-terminated or 2D Si phase [35]. Given the driving role that substrate interactions are expected to play in determining the properties of silicene in single or multiple layers, it is crucial to explore the effect of Si deposition on silicene grown upon on a variety of substrates.

Here we demonstrate that Si deposition onto monolayer silicene formed on ZrB_2 (0 0 0 1) thin films can cause substantial changes in the structural and electronic properties of the silicon layers. Using scanning tunnelling microscopy (STM), spectroscopy (STS), and low energy electron diffraction (LEED), we find that the deposition of Si onto the single-domain silicene/ZrB_2 surface [36] results in the formation of an atomically-thin layered silicon displaying substantially different electronic properties to both single layer, single-domain silicene and diamond-structured silicon. Most notably, angle resolved photoelectron spectroscopy (ARPES) measurements indicate that it has bands crossing the Fermi level, making it metallic. It is then shown that this new layered silicon retains its metallic nature upon further Si deposition. Such layered silicon could be used as an atomically-thin and atomically-sharp electrical contact to the single-domain silicene sheets formed on the ZrB_2 (0 0 0 1) surface [36] and possibly silicene formed on some other substrates. This result illustrates the surprisingly rich array of structural and electronic properties that 2D forms of Si can have.

2. Methods

ZrB_2 (0 0 0 1) thin films were grown on Si (1 1 1) wafers by ultrahigh vacuum (UHV) chemical vapour epitaxy [37]. Samples were then transferred in air to separate UHV systems for further characterization, with the silicene sheet being regenerated by annealing to 800 °C (by running a current through the sample or by electron beam bombardment of the back of the sample) for a few hours [11, 37]. STM imaging and spectroscopy measurements were performed at room temperature in an Omicron VT-STM.

Constant current topographic images were acquired using the STM feedback loop to change the tip height to maintain a set-point current I_0 at a set-point voltage V_0. Measurement of current I versus voltage V spectra via STS was performed by first specifying I_0 at an initial V_0 with the STM feedback loop closed to select an initial height for the tip above the surface and then measuring I versus V with the feedback loop open to keep the tip height fixed. Performing the same measurements at different set-point current/voltage combinations would scale the curves by a multiplicative constant, but would otherwise leave the shape of the spectrum unaffected. Since the absolute height of the tip above the surface cannot be determined directly, we essentially normalise the spectra by selecting the same I_0 and V_0 for all measurements.
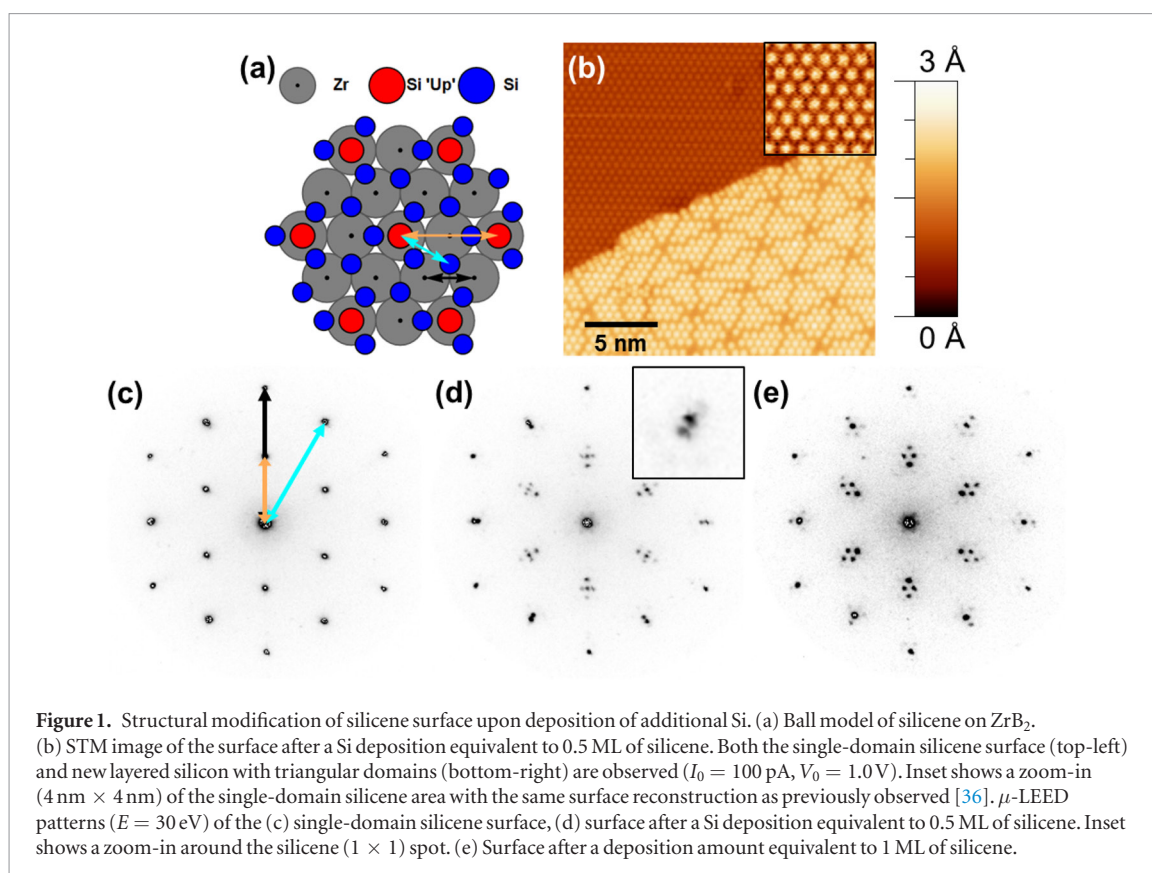
LEED patterns were obtained using the spectroscopic low-energy electron microscopy (Elmitec

SPE-LEEM) end-station located at BL U5UA of the National Synchrotron Light Source (NSLS, Brookhaven National Laboratory, Upton, NY, USA) operating in the μ-LEED mode using a 2 μm selected-area aperture. Si atoms have been deposited using a well-outgassed, resistively heated Si wafer as a source, onto samples radiatively heated to temperatures between 100 and 370 °C. For LEEM/μ-LEED measurements a Si flux corresponding to 2 MLs of silicene on ZrB_2 (1 ML = 1.73×10^{15} atoms cm^{-2}) per hour was employed. The flux was carefully calibrated using the contrast change in the dark field LEEM image of the Si(1 0 0) surface during the $(2 \times 1) \rightarrow (1 \times 2)$ transition upon Si deposition at the sample temperature of about 450 °C. In the STM measurements a higher Si flux of ~1.5 ML min^{-1} was used, calibrated by coverage analysis upon a Si (1 0 0) surface.

ARPES measurements were carried out at beamline BL13B of the Photon Factory synchrotron radiation facility located at the High-Energy Accelerator Research Organization (KEK, Tsukuba, Japan), using a photon energy of 43 eV. The energy resolution was better than 35 meV. The electric field vector of the light was at the fixed angle of 25° with respect to the photoelectron analyser.

3. Results and discussion

The spontaneous formation of silicene on the ZrB_2 (0 0 0 1) surface exhibits a highly ordered striped domain structure [11]. It has previously been demonstrated that additional Si atoms can be incorporated into the silicene sheet by depositing very small amounts of Si onto the surface [36]. The resulting single-domain silicene exhibits unaltered structural and electronic properties. Beyond this coverage, Si deposition onto a substrate with a temperature between 210 and 320 °C gives rise to structures similar to the one visible in the STM image in figure 1(b). Si depositions for substrate temperatures below 100 °C produced amorphous silicon structures, while at substrate temperatures of 370 °C the surface symmetry (as measured by LEED) did not progress beyond the pattern associated to the single-domain silicene surface. The STM image in figure 1(b) shows the surface after an amount of Si atoms equivalent to 0.5 ML of silicene has been deposited at a substrate temperature of 320 °C. In the top left-hand side of the image there is an area of single-domain silicene, within which the $(\sqrt{3} \times \sqrt{3})$-reconstruction of silicene on ZrB_2 (0 0 0 1) can be observed as a hexagonal array of circular protrusions; a model of this surface is shown in figure 1(a). The measured lattice constant of $a_{(\sqrt{3} \times \sqrt{3})} = 6.44 \pm 0.89$ Å is in good agreement with an expected value for the ZrB_2 (0 0 0 1)-(2 × 2) spacing of 6.37 Å, for ZrB_2 thin film epitaxially grown on Si(1 1 1) substrate [37–39]. In the lower section of the image there is an atomically sharp transition to a new 2D Si structure, whose surface in STM imaging is higher than that of single-domain silicene. The atomic motif is found

Figure 1. Structural modification of silicene surface upon deposition of additional Si. (a) Ball model of silicene on ZrB_2. (b) STM image of the surface after a Si deposition equivalent to 0.5 ML of silicene. Both the single-domain silicene surface (top-left) and new layered silicon with triangular domains (bottom-right) are observed ($I_0 = 100\,pA$, $V_0 = 1.0\,V$). Inset shows a zoom-in (4 nm × 4 nm) of the single-domain silicene area with the same surface reconstruction as previously observed [36]. μ-LEED patterns ($E = 30\,eV$) of the (c) single-domain silicene surface, (d) surface after a Si deposition equivalent to 0.5 ML of silicene. Inset shows a zoom-in around the silicene (1 × 1) spot. (e) Surface after a deposition amount equivalent to 1 ML of silicene.

to have a lattice constant slightly larger than that of the ($\sqrt{3} \times \sqrt{3}$)-reconstruction of silicene, 6.52 ± 0.96 Å. However, it displays a dramatically different quasi-ordered triangular-domain structure. As has been seen for the striped-domain boundaries of spontaneously-formed silicene [11], atoms adjacent to the domain boundaries are observed to be mobile at room temperature. The atom mobility is directly observed by STM as a hopping of protrusions from one domain to the other. In the triangular-domain surface, the hopping of atoms across the domain boundaries causes significant motion in the sides of the domains from scan to scan, which take approximately 10 min to complete, yet the dark vertices remain approximately fixed. The size of the domains varies from approximately 2 nm to 4 nm.

The apparent height of the new layered silicon relative to the single-domain silicene sheet as measured by STM is found to be heavily bias dependent, ranging approximately linearly from 0.30 nm to 0.15 nm over the voltage range of −1 V to 1 V (see supporting figure S1 (stacks.iop.org/TDM/4/021015/mmedia)). This indicates that part of the apparent height difference arises from differences in the electronic structure of the two layers. Importantly, this distance is less than that of the ZrB_2 step height of 0.35 nm [39], and less than predicted values for multi-layer silicene [28, 40, 41]. It however suggests the formation of a layered silicon structure thicker than silicene. The new silicon structure is observed to grow as a 2D layer across the surface without creating silicene-denuded areas in the vicinity. This is in contrast with the case of Si deposition beyond a monolayer of silicene on Ag(1 1 1) at higher substrate

temperatures, in which either a ($1/2\,\sqrt{21} \times 1/2\,\sqrt{21}$) structure [42] or a ($4/\sqrt{3} \times 4/\sqrt{3}$) structure [43] is formed; both of these are considered to consist of layers of diamond-structured, bulk-like Si.

The deposition of Si atoms was monitored by LEED. The single-domain silicene LEED pattern is composed of three significant contributions: the ZrB_2 (0 0 0 1)-(1 × 1), silicene (1 × 1), and silicene ($\sqrt{3} \times \sqrt{3}$) R30° spots, highlighted by the black, blue, and orange arrows respectively in figure 1(c). In figures 1(d) and (e), the LEED patterns after 0.5 MLs and 1.0 MLs of Si deposition, respectively, are shown. The LEED patterns point out the evolution of the silicene-related spots. The complete vanishing of the spots related to silicene (1 × 1) after deposition of 1 ML, while those of ZrB_2 (0 0 0 1)-(1 × 1) remain visible, indicate that the silicene layer underneath does not survive upon the formation of the new layered silicon. The concomitant appearance of spots at inward positions suggests that the new layered silicon has a lattice parameter approximately 5% larger than that of silicene on the ZrB_2 (0 0 0 1) surface. It can therefore be conceived that, just like silicene on ZrB_2, the array of protrusions observed in the STM images is the result of the ($\sqrt{3} \times \sqrt{3}$) reconstruction of a layered silicon that appears with a slightly enlarged lattice constant. The new silicon surface lattice constant of 6.52 ± 0.96 Å is also comparable to the in-plane lattice constant of ($\sqrt{3} \times \sqrt{3}$)-reconstructed multi-layer silicene grown on Ag(1 1 1) (6.477 ± 0.015 Å) [35].

The small increase of the lattice parameter between silicene and the layered silicon suggests that the
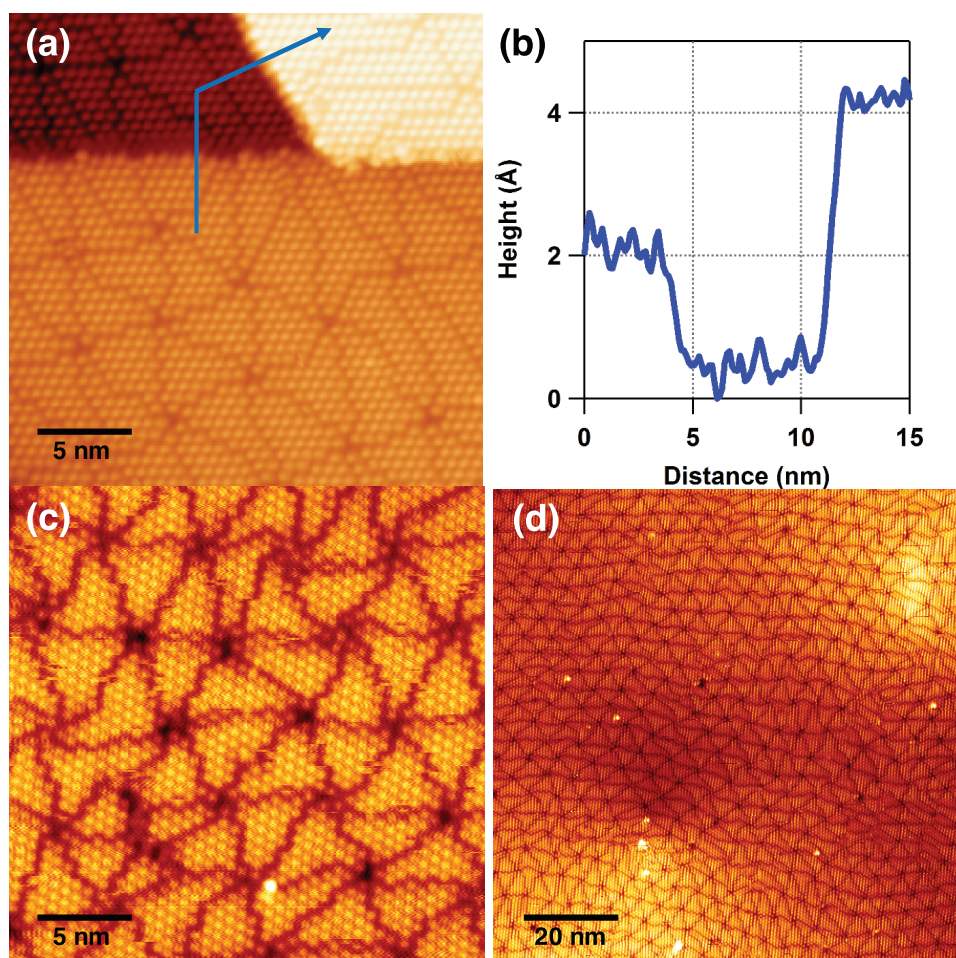
Figure 2. Layered silicon surfaces after significant Si deposition. (a) STM image of the surface after Si deposition equivalent to 1.5 ML of silicene. Three layers can be observed, at the lowest (top left) a layered silicon lays ~0.35 nm (a ZrB_2 step) below another ZrB_2 (0 0 0 1) terrace also with a layered silicon grown on top (top right). In the bottom two-third of the image, additional layer is observed ~0.15 nm above the lowest layered silicon ($I_0 = 50$ pA, $V_0 = 1.0$ V). (b) Height profile of the blue line in (a). High resolution ($I_0 = 50$ pA, $V_0 = 1.0$ V) (c) and large scale ($I_0 = 20$ pA, $V_0 = -1.0$ V) (d) STM images of the surface after a deposition amount equivalent to 9 ML of silicene.

triangular domain structure arises from a new epitaxial relationship between the silicon layers and the ZrB_2 substrate with a larger-scale supercell. The electronic properties observed may be influenced by the strain in this new layered silicon, a property known to be important in the case of graphene [44, 45]. In LEED the triangle domain structure is reflected mostly by the 'diamond' feature made of satellite spots appearing around the ($\sqrt{3} \times \sqrt{3}$) spot of silicene. The flexibility of the silicene structure is demonstrated by the possible incorporation of Si atoms into the boundaries of the stripe-domains [36, 46]. In contrast, for the new layered silicon, the increased rigidity of the Si bonding may make the lattice matching between the ZrB_2 (0 0 0 1)-(2 × 2) and Si ($\sqrt{3} \times \sqrt{3}$)-reconstruction energetically less favourable.

When the amount of deposited Si is increased above 1 ML, the LEED pattern does not show noticeable change from that shown in figure 1(e). Figure 2(a) shows an STM image of the layered Si surface across a ZrB_2 terrace step after a 1.5 ML Si deposition. The highest layer in the top right of the image is 0.35 nm (a ZrB_2 step) above the lowest layer (top left of the image)

on the terrace below. In this image, we see a rare step in between these terraces with an apparent step height of 0.15 nm (step height profile shown in figure 2(b)); this apparent height is not expected to be significantly sensitive to the applied voltage owing to the similarity in electronic structure (discussed below). As with the step height of the layered silicon above the single-domain silicene surface, the interlayer spacing of 0.15 nm is smaller than would be expected for weak van der Waals interactions between layers or even those for densely packed metals. For the surface after a Si deposition amount equivalent to 2 ML of silicene, the quasi-ordered triangular domain size increases by approximately 30% in comparison to the layered silicon surface formed after depositing 1 ML of Si.

The same quasi-ordered triangular domain structure with increased domain size is observed by STM after a 9 ML Si deposition (figure 2(c)), which suggests that the new layered silicon is stable and does not transition to diamond-structured silicon, even after depositing significant amounts of Si atoms. We note here that although 9 MLs of Si were deposited, the actual thickness of the layered silicon is unknown. In addition, we
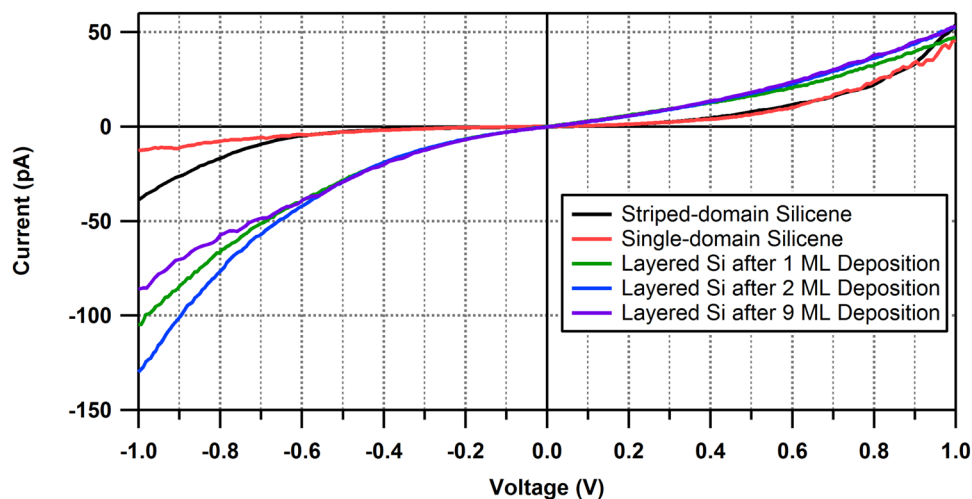
Figure 3. Scanning tunnelling spectra of silicene and layered silicon surfaces. $I(V)$ curves taken at room temperature above the spontaneously-formed stripe-domain silicene (black), single-domain silicene (red), layered silicon after 1 ML deposition (green), 2 ML deposition (additional layer in figure 2(a)) (blue), and 9 ML deposition (purple). ($I_0 = 50$ pA, $V_0 = 1.0$ V).

note that for these significant amounts of Si deposition, the surface remains atomically flat over large areas (figure 2(d)). However, upon heating to 800 °C, the striped domain silicene is regenerated, indicating the metastability of the layered silicon and single-domain silicene with respect to this surface; this may occur either through desorption of the additional Si layers or through clustering in confined areas on the surface.

The electronic properties of the layered silicon have been investigated by room temperature STS and ARPES measurements. Figure 3 compares the tunnelling current as a function of applied bias voltage $I(V)$ as measured on spontaneously-formed silicene; single-domain silicene; layered silicon formed by Si deposition upon silicene (figure 2(a)); and the surface after a 9 ML Si deposition. There is little difference in the electronic structure between the single-layer silicene surfaces (red and black) within the range of -0.6–0.9 V. Furthermore, all surfaces have an approximately linear $I(V)$ curve within ± 0.1 V of the Fermi level and therefore it is not possible to make a definitive statement on their relative conductance from STS measurements. However, a clear difference is observed in the electronic structure between the silicene (black and red) and those of the layered silicon surfaces (green, blue, and purple), distinguished by the far greater relative current at negative bias (filled states) compared to positive bias (empty states).

ARPES measurements taken along the ZrB_2 $(0\,0\,0\,1)$-(1×1) $\Gamma - M - \Gamma$ direction reveal the nature of the changes in the electronic structure in the new layered silicon (figure 4). In comparison to the previously reported equivalent ARPES measurements on the stripe-domain [11] and single-domain [36] silicene surfaces, the new layered silicon is found to have additional bands crossing the Fermi level in the vicinity of the ZrB_2 $(0\,0\,0\,1)$-(1×1) M-point (vertical white line in figure 4), which corresponds to the K-point of the stripe- and single-domain silicene surfaces on ZrB_2.
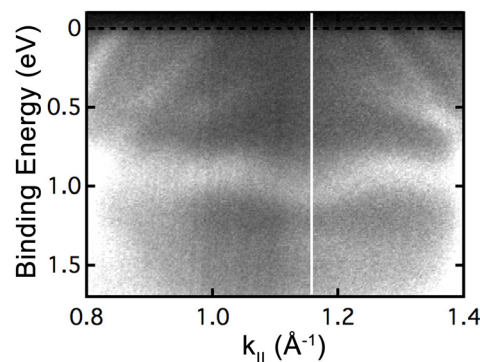
Figure 4. Valence electronic structure of new layered silicon. ARPES spectra taken along the ZrB_2 $(0\,0\,0\,1)$ $\Gamma - M - \Gamma$ direction in the vicinity of the M-point which corresponds to the K-point of single-domain (1×1) silicene on ZrB_2. Spectra reveal a pair of bands symmetrically separated in the vicinity of the ZrB_2 $(0\,0\,0\,1)$-(1×1) M-point (white vertical line) that cross the Fermi level.

The greater density of states due to the additional bands crossing at the Fermi level qualitatively suggest that the new layered silicon is metallic and that it will be more conductive than silicene. Future in-plane conductance measurements may quantify the precise enhancement of conductance.

Although it is not possible to resolve the complete atomic configuration of the new layered silicon, both LEED and STM measurements indicate that a three-fold symmetric unit cell is retained that may result from a honeycomb structure with a lattice parameter that is larger than that of the bare silicene. Further investigation will be required to differentiate between various possible configurations, including a bilayer of silicene or a previously unseen layered phase or surface reconstruction. We note that the apparent interlayer spacing of 0.15 nm is different from the 0.24–0.42 nm spacing expected for an isolated bilayer of silicene [28, 40, 41], though the sensitivity of silicene to the supporting substrate leaves open the possibility for a novel surface

reconstruction of a silicene multilayer structure. It is also noted that although surface segregation of Zr or B to the surface cannot be ruled out, it is considered to be unlikely due to the high thermal stability or ZrB_2 [47] and the lack of a band gap as would be expected for B-terminated silicon [48, 49].

A variety of silicon nanostructures are known, the properties of which vary greatly with crystallographic face [50], doping [51, 52], particle size [53], and morphology [53–55]. Application of significant pressures (>10 GPa) to silicon with diamond structure induces a number of allotropic phase transitions to metallic forms of silicon [56–58]. Interestingly, the layered silicon observed in this study, in stark contrast to silicene on ZrB_2 and also to semiconducting diamond-structured bulk silicon, is also metallic. The formation of this atomically sharp transition from silicene to a metallic 2D layered silicon could prove useful as a contact to the single-domain silicene formed on ZrB_2 surface, where the 2D growth of the silicon overlayers could still allow for the use of further encapsulating layers.

4. Conclusion

In conclusion, it has been shown that the deposition of Si atoms onto silicene formed on a ZrB_2 surface results in the formation of a new 2D silicon crystal with dramatically different structural and electronic properties. STM and LEED have shown that there is a restructuring of the silicon layers as the new layered silicon is grown upon the single-domain silicene surface. LEED measurements suggest that there is still a silicon lattice with a similar lattice constant (0.39 nm) to the silicene/ZrB_2 (1×1) unit cell (0.36 nm), which qualitatively describes the formation of the triangular domain boundaries. The epitaxial growth of this new, metallic layered silicon could allow for the direct and unobtrusive contacting to the single-domain silicene sheet, an important step towards improving silicene-based devices. For this, future studies should explore the impact of the domain boundaries on the in-plane conductivity in detail. In addition, further investigations into the atomic scale geometry of this new surface will be required to better understand the origin of the new bands crossing the Fermi level as observed by ARPES.

Data Availability

Experimental data that support the findings of the paper are available at https://doi.org/10.6084/m9.figshare.c.3688366. Additional information on the experimental data can be obtained by contacting the authors.

Acknowledgments

References

[1] Guzmán-Verri G and Lew Yan Voon L 2007 Electronic structure of silicon-based nanostructures *Phys. Rev.* B **76** 75131

[2] Takeda K and Shiraishi K 1994 Theoretical possibility of stage corrugation in Si and Ge analogs of graphite *Phys. Rev.* B **50** 14916–22

[3] Liu C-C, Feng W and Yao Y 2011 Quantum Spin Hall effect in silicene and two-dimensional germanium *Phys. Rev. Lett.* **107** 76802

[4] Liu C-C, Jiang H and Yao Y 2011 Low-energy effective Hamiltonian involving spin-orbit coupling in silicene and two-dimensional germanium and tin *Phys. Rev.* B **84** 195430

[5] Tahir M and Schwingenschlögl U 2012 Magnetocapacitance of an electrically tunable silicene device *Appl. Phys. Lett.* **101** 132412

[6] Drummond N D, Zólyomi V and Fal'ko V I 2012 Electrically tunable band gap in silicene *Phys. Rev.* B **85** 75423

[7] Ni Z, Liu Q, Tang K, Zheng J, Zhou J, Qin R, Gao Z, Yu D and Lu J 2012 Tunable bandgap in silicene and germanene *Nano Lett.* **12** 113–8

[8] Tahir M and Schwingenschlögl U 2013 Valley polarized quantum Hall effect and topological insulator phase transitions in silicene *Sci. Rep.* **3** 1075

[9] Tao L, Cinquanta E, Chiappe D, Grazianetti C, Fanciulli M, Dubey M, Molle A and Akinwande D 2015 Silicene field-effect transistors operating at room temperature *Nat. Nanotechnol.* **10** 227–31

[10] Vogt P, De Padova P, Quaresima C, Avila J, Frantzeskakis E, Asensio M C, Resta A, Ealet B and Le Lay G 2012 Silicene: compelling experimental evidence for graphenelike two-dimensional silicon *Phys. Rev. Lett.* **108** 155501

[11] Fleurence A, Friedlein R, Ozaki T, Kawai H, Wang Y and Yamada-Takamura Y 2012 Experimental evidence for epitaxial silicene on diboride thin films *Phys. Rev. Lett.* **108** 245501

[12] Meng L, Wang Y, Zhang L, Du S, Wu R, Li L, Zhang Y, Li G, Zhou H, Hofer W A and Gao H-J 2013 Buckled silicene formation on Ir(1 1 1) *Nano Lett.* **13** 685–90

[13] Chen L, Liu C-C, Feng B, He X, Cheng P, Ding Z, Meng S, Yao Y and Wu K 2012 Evidence for Dirac fermions in a honeycomb lattice based on silicon *Phys. Rev. Lett.* **109** 56804

[14] Aizawa T, Suehara S and Otani S 2014 Silicene on Zirconium Carbide (1 1 1) *J. Phys. Chem.* C **118** 23049–57

[15] Aizawa T, Suehara S and Otani S 2015 Phonon dispersion of silicene on ZrB_2 (0 0 0 1) *J. Phys.: Condens. Matter* **27** 305002

[16] Berger C *et al* 2006 Electronic confinement and coherence in patterned epitaxial graphene *Science* **312** 1191–6

[17] de Heer W A *et al* 2007 Epitaxial graphene *Solid State Commun.* **143** 92–100

[18] Zhou S Y, Gweon G-H, Fedorov A V, First P N, de Heer W A, Lee D-H, Guinea F, Castro Neto A H and Lanzara A 2007

Substrate-induced bandgap opening in epitaxial graphene *Nat. Mater.* **6** 770–5

[19] Varchon F *et al* 2007 Electronic structure of epitaxial graphene layers on SiC: effect of the substrate *Phys. Rev. Lett.* **99** 126805

[20] Luk'yanchuk I and Kopelevich Y 2004 Phase analysis of quantum oscillations in graphite *Phys. Rev. Lett.* **93** 166402

[21] Gao N, Li J C and Jiang Q 2014 Bandgap opening in silicene: effect of substrates *Chem. Phys. Lett.* **592** 222–6

[22] Lin C-L, Arafune R, Kawahara K, Kanno M, Tsukahara N, Minamitani E, Kim Y, Kawai M and Takagi N 2013 Substrate-induced symmetry breaking in silicene *Phys. Rev. Lett.* **110** 76801

[23] Ohta T, Bostwick A, Seyller T, Horn K and Rotenberg E 2006 Controlling the electronic structure of bilayer graphene *Science* **313** 951–4

[24] Ohta T, Bostwick A, McChesney J, Seyller T, Horn K and Rotenberg E 2007 Interlayer interaction and electronic screening in multilayer graphene investigated with angle-resolved photoemission spectroscopy *Phys. Rev. Lett.* **98** 206802

[25] Zhang Y, Tang T-T, Girit C, Hao Z, Martin M C, Zettl A, Crommie M F, Shen Y R and Wang F 2009 Direct observation of a widely tunable bandgap in bilayer graphene *Nature* **459** 820–3

[26] Mak K F, Lee C, Hone J, Shan J and Heinz T F 2010 Atomically thin MoS_2: a new direct-gap semiconductor *Phys. Rev. Lett.* **105** 136805

[27] Splendiani A, Sun L, Zhang Y, Li T, Kim J, Chim C Y, Galli G and Wang F 2010 Emerging photoluminescence in monolayer MoS_2 *Nano Lett.* **10** 1271–5

[28] Liu J and Zhang W 2013 Bilayer silicene with an electrically-tunable wide band gap *RSC Adv.* **3** 21943

[29] Liu F, Liu C-C, Wu K, Yang F and Yao Y 2013 d + id' Chiral superconductivity in bilayer silicene *Phys. Rev. Lett.* **111** 66804

[30] Ezawa M 2012 Quasi-topological insulator and trigonal warping in gated bilayer silicene *J. Phys. Soc. Japan* **81** 104713

[31] De Padova P *et al* 2013 The quasiparticle band dispersion in epitaxial multilayer silicene *J. Phys.: Condens. Matter* **25** 382202

[32] Vogt P, Capiod P, Berthe M, Resta A, De Padova P, Bruhn T, Le Lay G and Grandidier B 2014 Synthesis and electrical conductivity of multilayer silicene *Appl. Phys. Lett.* **104** 21602

[33] Mannix A J, Kiraly B, Fisher B L, Heram M C and Guisinger N P 2014 Silicon growth at the two-dimensional limit on Ag(1 1 1) *ACS Nano* **8** 7538–47

[34] Shirai T, Shirasawa T, Hirahara T, Fukui N, Takahashi T and Hasegawa S 2014 Structure determination of multilayer silicene grown on Ag(1 1 1) films by electron diffraction: evidence for Ag segregation at the surface *Phys. Rev. B* **89** 241403

[35] De Padova P, Generosi A, Paci B, Ottaviani C, Quaresima C, Olivieri B, Salomon E, Angot T and Le Lay G 2016 Multilayer silicene: clear evidence *2D Mater.* **3** 31011

[36] Fleurence A, Gill T G, Friedlein R, Sadowski J T, Aoyagi K, Copel M, Tromp R M, Hirjibehedin C F and Yamada-Takamura Y 2016 Single-domain epitaxial silicene on diboride thin films *Appl. Phys. Lett.* **108** 151902

[37] Yamada-Takamura Y, Bussolotti F, Fleurence A, Bera S and Friedlein R 2010 Surface electronic structure of ZrB_2 buffer layers for GaN growth on Si wafers *Appl. Phys. Lett.* **97** 73109

[38] Roucka R, An Y, Chizmeshya A V G, Tolle J, Kouvetakis J, D'Costa V R, Menendez J and Crozier P 2006 Epitaxial semimetallic $Hf_xZr_{1-x}B_2$ templates for optoelectronic integration on silicon *Appl. Phys. Lett.* **89** 242110

[39] Fleurence A and Yamada-Takamura Y 2011 Scanning tunneling microscopy investigations of the epitaxial growth of ZrB_2 on Si(1 1 1) *Phys. Status Solidi* **8** 779–83

[40] Fu H, Zhang J, Ding Z, Li H and Meng S 2014 Stacking-dependent electronic structure of bilayer silicene *Appl. Phys. Lett.* **104** 131904

[41] Naji S, Khalil B, Labrim H, Bhihi M, Belhaj A, Benyoussef A, Lakhal M and El Kenz A 2014 Interdistance effects on flat and buckled silicene like-bilayers *J. Phys. Conf. Ser.* **491** 12006

[42] Acun A, Poelsema B, Zandvliet H J W and Van Gastel R 2013 The instability of silicene on Ag(1 1 1) *Appl. Phys. Lett.* **103** 263119

[43] Kawahara K, Shirasawa T, Lin C-L, Nagao R, Tsukahara N, Takahashi T, Arafune R, Kawai M and Takagi N 2016 Atomic structure of 'multilayer silicone' grown on Ag(1 1 1): dynamical low energy electron diffraction analysis *Surf. Sci.* **651** 70–5

[44] Choi S-M, Choi S-M, Jhi S-H, Jhi S-H, Son Y-W and Son Y-W 2010 Effects of strain on electronic properties of graphene *Phys. Rev. B* **81** 081407

[45] Levy N, Burke S A, Meaker K L, Panlasigui M, Zettle A, Guinea F, Castro Neto A H and Crommie M F 2010 Strain-induced pseudo-magnetic fields greater than 300 T in graphene nanobubbles *Science* **329** 544–7

[46] Lee C-C, Fleurence A, Friedlein R, Yamada-Takamura Y and Ozaki T 2014 Avoiding critical-point phonon instabilities in two-dimensional materials: the origin of the stripe formation in epitaxial silicene *Phys. Rev. B* **90** 241402

[47] Fahrenholtz W G, Hilmas G E, Talmy I G and Zaykoski J A 2007 Refractory diborides of zirconium and hafnium *J. Am. Ceram. Soc.* **90** 1347–64

[48] Grehk T M, Martensson P and Nicholls J M 1992 Occupied and unoccupied surface states on the Si(1 1 1) $\sqrt{3} \times \sqrt{3} \times \sqrt{3}$: B surface *Phys. Rev. B* **46** 2357–63

[49] Berthe M *et al* 2006 Electron transport via local polarons at interface atoms *Phys. Rev. Lett.* **97** 206801

[50] Waltenburg H N and Yates J T 1995 Surface chemistry of silicon *Chem. Rev.* **95** 1589–673

[51] Yu P Y and Cardona M 2005 *Fundamentals of Semiconductors: Physics and Material Properties* (Berlin: Springer)

[52] McCluskey M D and Haller E E 2012 *Dopants and Defects in Semiconductors* (Boca Raton, FL: Taylor and Francis)

[53] Puzder A, Williamson A J, Grossman J C and Galli G 2002 Surface chemistry of silicon nanoclusters *Phys. Rev. Lett.* **88** 97401

[54] Cullis A G, Canham L T and Calcott D J 1997 The structural and luminescence properties of porous silicon *J. Appl. Phys.* **82** 909–65

[55] Rurali R 2010 Colloquium: structural, electronic, and transport properties of silicon nanowires *Rev. Mod. Phys.* **82** 427–49

[56] Wentorf R H and Kasper J S 1963 Two new forms of silicon *Science* **139** 338

[57] Yin M T and Cohen M 1982 Theory of static structural properties, crystal stability, and phase transformations: application to Si and Ge *Phys. Rev. B* **26** 5668–87

[58] Sorella S, Casula M, Spanu L and Corso A D 2011 *Ab initio* calculations for the β-tin diamond transition in silicon: comparing theories with experiments *Phys. Rev. B* **75119** 1–12